Human Molecular Genetics, 2013, Vol. 22, No. 15 **3077–3092**
doi:10.1093/hmg/ddt164
Advance Access published on April 11, 2013

De-repression of FOXO3a death axis by microRNA-132 and -212 causes neuronal apoptosis in Alzheimer's disease

Hon-Kit Andus Wong[1,†], Tatiana Veremeyko[1,†], Nehal Patel[2], Cynthia A. Lemere[1], Dominic M. Walsh[3], Christine Esau[4], Charles Vanderburg[2] and Anna M. Krichevsky[1,*]

[1]Center for Neurologic Diseases, Brigham and Women's Hospital and Harvard Medical School, Harvard Institutes of Medicine, Boston, MA 02115, USA, [2]Harvard NeuroDiscovery Center, Massachusetts General Hospital and Harvard Medical School, Building 114, Charlestown, MA 02129, USA, [3]Laboratory for Neurodegenerative Research, Center for Neurologic Diseases, Brigham and Women's Hospital, Harvard Institutes of Medicine, Boston, MA, USA and [4]Regulus Therapeutics, 3545 John Hopkins Ct, San Diego, CA 92121, USA

Received December 10, 2012; Revised March 21, 2013; Accepted April 5, 2013

Alzheimer's disease (AD) is a multifactorial and fatal neurodegenerative disorder for which the mechanisms leading to profound neuronal loss are incompletely recognized. MicroRNAs (miRNAs) are recently discovered small regulatory RNA molecules that repress gene expression and are increasingly acknowledged as prime regulators involved in human brain pathologies. Here we identified two homologous miRNAs, miR-132 and miR-212, downregulated in temporal cortical areas and CA1 hippocampal neurons of human AD brains. Sequence-specific inhibition of miR-132 and miR-212 induces apoptosis in cultured primary neurons, whereas their overexpression is neuroprotective against oxidative stress. Using primary neurons and PC12 cells, we demonstrate that miR-132/212 controls cell survival by direct regulation of PTEN, FOXO3a and P300, which are all key elements of AKT signaling pathway. Silencing of these three target genes by RNAi abrogates apoptosis caused by the miR-132/212 inhibition. We further demonstrate that mRNA and protein levels of PTEN, FOXO3a, P300 and most of the direct pro-apoptotic transcriptional targets of FOXO3a are significantly elevated in human AD brains. These results indicate that the miR-132/miR-212/PTEN/FOXO3a signaling pathway contributes to AD neurodegeneration.

INTRODUCTION

Alzheimer's disease (AD) is a progressive neurodegenerative disorder and the most common form of age-associated dementia. It represents the fourth cause of death in industrialized societies, and by 2050, it is estimated that more than 100 million people will suffer from AD (1). The significant synaptic and neuronal loss in the basal forebrain, hippocampus and cortex of the human brain in AD is believed to lead to manifestations of clinical symptoms such as cognitive decline. However, owing to the slowly progressing nature of neuronal loss in AD, the study of neuronal death has been challenging and the cause and fundamental mechanisms of neuronal cytotoxicity remain highly controversial (2). Delineating the mechanisms of neuronal death, therefore, has been one of the main focuses in the AD field with an aim to apply novel therapeutics at the earliest possible time window to prevent neuronal loss. However, no effective therapies have yet been found to prevent neuronal loss and the subsequent cognitive impairments.

The recently discovered microRNAs (miRNAs) may offer a novel approach to reveal previously undescribed regulatory mechanisms of cell death in AD. miRNAs are short non-protein-coding RNA molecules that are abundantly expressed in the brain (3–6). They function as negative regulators of gene expression at the posttranscriptional level by repressing

*To whom correspondence should be addressed at: Center for Neurologic Diseases, Brigham and Women's Hospital and Harvard Medical School, Harvard Institutes of Medicine (HIM), 77 Avenue Louis Pasteur, Boston, MA 02115, USA. Tel: +1 6175255195; Fax: +1 6175255305; Email: akrichevsky@rics.bwh.harvard.edu
†These authors contributed equally to this study.

translation and/or promoting mRNA degradation (7,8). Indeed, changes of miRNA expression have recently been shown to be associated with a number of central nervous system disorders, including AD (9,10). miRNAs may target the key disease-associated genes such as amyloid precursor protein (APP) (11–18) or BACE1 (19–23) and thus potentially modulate the levels of toxic Aβ species and the subsequent neuronal death. However, the data on miRNA(s) that directly regulate cell death pathways in AD human neurons have only begun to emerge (23,24).

To investigate the miRNA-mediated regulation in AD pathogenesis and identify specific changes in the miRNA levels in the neuronal populations that are most prone to AD, we profiled miRNA expression in AD tissues and laser-captured hippocampal neurons from AD and age-matched control brains. Compared with the controls, the expression of two homolog miRNAs, miR-132 and miR-212, was markedly and significantly downregulated in AD neurons. These activity-regulated miRNAs are required for normal dendrite maturation in newborn neurons (25) and affect dendritic morphology in mature neurons (26). Here we report that miR-132/212 also controls survival of neural cells by direct regulation of three proteins associated with cell death: Phosphatase and Tensin Homolog (PTEN), Forkhead Box O3a (FOXO3a), and E1A binding protein p300 (P300). Furthermore, expression levels of PTEN, FOXO3a, P300, as well as most of the direct transcriptional targets of FOXO3a, are elevated in AD brains. These results indicate that miR-132/212 modulates neuronal survival and implicate PTEN/AKT/FOXO3a-associated death-signaling axis in AD neurodegeneration.

RESULTS

Downregulation of miR-132/212 in AD neurons

To identify miRNAs that are deregulated in the progression of AD, we profiled 40 selected brain-enriched miRNAs from temporal cortex specimens of patients with the Braak III (mild AD) and Braak VI (severe AD) neuro-pathology and age-matched controls ($n = 6$ per group) by multiplex qRT–PCR assays. We utilized formalin-fixed brain tissues from the Harvard Brain Tissue Resource Center, and the presence of Aβ and NFTs in adjacent brain sections was confirmed by immunohistochemistry. Among these miRNAs, we found that expression levels of two brain-enriched miRNAs, miR-132 and miR-212, were markedly and significantly reduced in AD. These results were confirmed by the miRNA-specific singleplex qRT–PCR analysis of larger patient cohorts ($n = 14–16$ per group) (Fig. 1A and B, and case details in Supplementary Material, Table S1). There was a 1.4 ($^{*}P = 0.041$) and 3.8 ($^{**}P < 0.0001$)-fold decrease in Braak III/IV and Braak VI stages for miR-132 expression (Fig. 1B left), and a 1.5 ($^{*}P = 0.022$) and 2.7 ($^{**}P < 0.0001$)-fold decrease in Braak III/IV and Braak VI for that of miR-212 (Fig. 1B right), compared with the age-matched controls. To further investigate whether the reduction of miR-132 and miR-212 levels in AD brains was due specifically to their downregulation in neurons (rather than a smaller proportion of neurons in AD brains relative to normal specimens), we laser-captured neuronal cell bodies from the hippocampal CA1 regions of Braak III and Braak VI brains ($n = 5$ per group) and analyzed the neuronal expression of miR-132 and miR-212 [see Fig. 1C and Supplementary Material, Fig. S1 for some laser capture microdissection (LCM) details]. Consistent with the changes that we observed in the temporal cortex, the expression of miR-132 (Fig. 1C, left) and miR-212 (right) also tended to be decreased in hippocampal neurons obtained from the CA1 region of Braak VI brains, the most affected area with the greatest extent of neuronal death in AD. Although statistically insignificant due to a small number of laser-captured samples analyzed, and possibly also lack of neuronal processes in the analyzed material, the observed trend indicated that miR-132 and miR-212 were downregulated in hippocampal neurons in AD.

To monitor the expression of miR-132 and miR-212 in a genetically defined AD background, we employed APPswe, PSEN1dE9 (APP PS1) mice. These double-transgenic mice express a chimeric mouse/human APP/APP (Mo/HuAPP695swe) and a mutant human presenilin/PSEN 1 (PS1-dE9) in CNS neurons (27). In human, both mutations are associated with early-onset Alzheimer's disease. Analysis of expression of miR-132 and miR-212 revealed a significant downregulation of both miRNAs in the pathological areas (including hippocampus) of 6-month-old mice at the onset of Aβ deposition and behavioral defects (Fig. 1E). These data further support the notion that miR-132 and miR-212 downregulation is an important element of AD pathogenesis.

Loss of miR-132/212 causes neuronal apoptosis

miR-132 and miR-212 are functionally similar miRNAs encoded in the same genomic locus in all vertebrates (human chr.17p13.3). The levels of miR-132 and miR-212 correlate in human temporal cortex specimens in normal and AD brains (Fig. 1D), which suggests their co-expression and simultaneous downregulation in AD. They share a seed, the 5′ region that is especially important for a target binding, and therefore likely regulate similar populations of mRNA targets. miR-132 is relatively well-characterized as one of the brain-enriched miRNAs that primarily modulates neuronal plasticity through CREB-dependent signaling (28) both *in vitro* (29) and *in vivo* (30,31). It has been shown that deletion of hippocampal miR-132/212 *in vivo* leads to decreased dendritic length and arborization (25). As there is a significant loss of neurons and reduction of miR-132/212 levels in the hippocampal neurons of CA1 region in AD (Fig. 1C), we hypothesized that, in addition to its critical function in regulating dendritic length and spine density, miR-132/212 may have a direct function in maintaining neuronal survival, and its decreased levels may contribute to neuron death. To investigate their role in neuronal survival, we inhibited miR-132 and/or miR-212 in primary hippocampal and cortical neurons with sequence-specific antisense oligonucleotide inhibitors. We achieved transfection efficiency of ∼90–95% for both young and mature neurons (Supplementary Material, Fig. S2). Highly potent, stable and non-toxic 2′-*O*-methoxyethyl oligonucleotides (2′-*O*-MOE) (32,33) enabled long-lasting inhibition of miR-132 or miR-212 over at least 14 days (Supplementary Material, Fig. S3). Inhibition of miR-132 or miR-212 in both cortical and hippocampal neurons increased apoptotic cell death significantly, as reflected by terminal deoxynucleotidyl transferase dUTP nick end labeling (TUNEL) assay (Fig. 2A–C). The strongest 6–8-fold effect has been observed in mature

A

Age	Gender	PMI (hrs)	Diagnosis	Sample	Cases (n)
76.5 ± 4.7	10M/6F	18.3 ± 8.2	NDAR/controls	Temporal cortex	16
81.4 ± 7.0	5M/9F	21.6 ± 7.5	Braak III/IV	Temporal cortex	14
81.7 ± 5.7	6M/10F	16.0 ± 7.9	Braak VI	Temporal cortex	16

PMI: Post Mortem Interval
NDAR: No Diagnostic Abnormality Recognized
All data are mean ± standard deviation

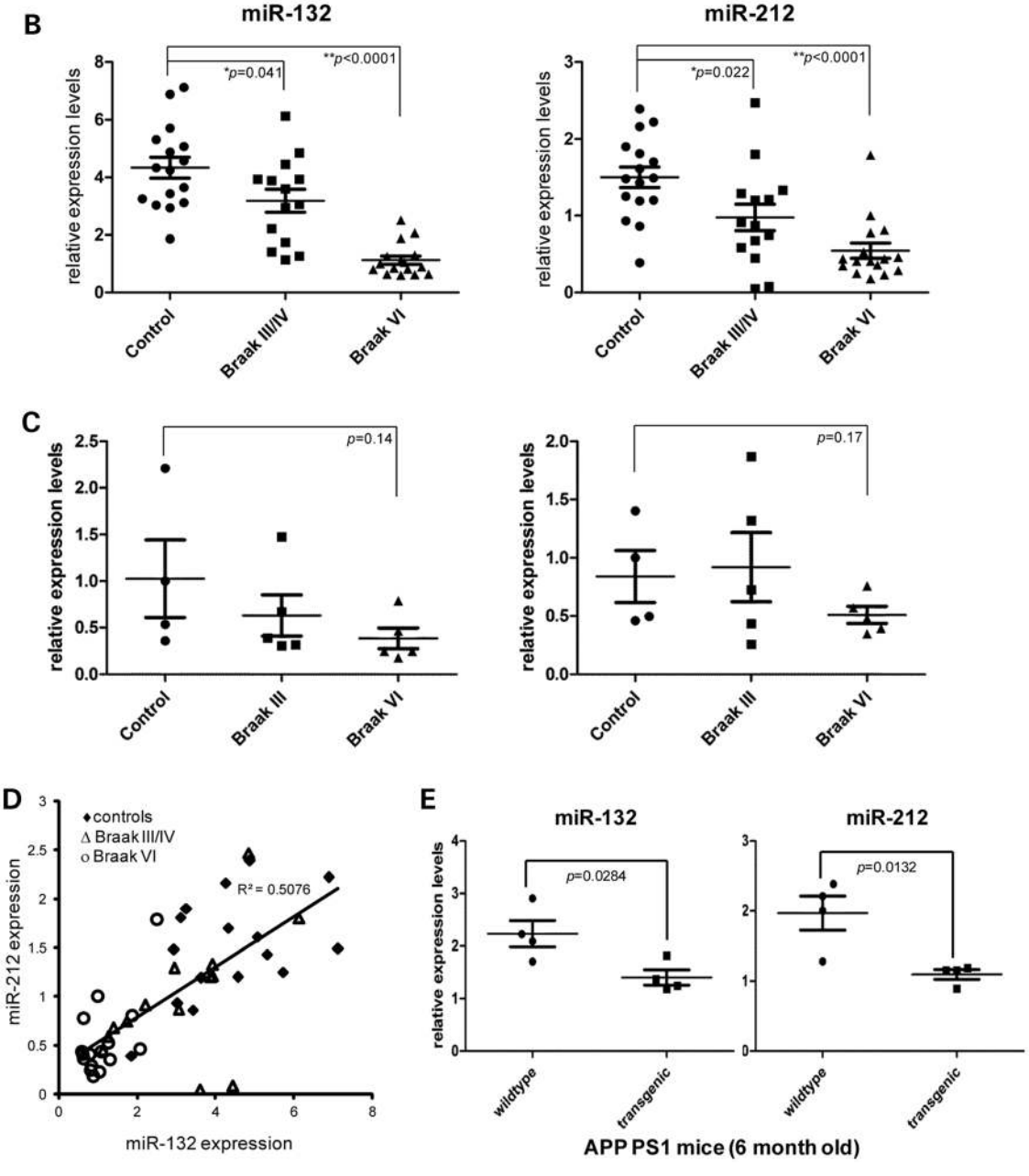

Figure 1. Downregulation of miR-132 and miR-212 expression in the AD brain. (**A**) The table summarizes the sample information used in this study. Please refer to Supplementary Material, Table S1 for more details. (**B**) Expression of miR-132 (left) and miR-212 (right) in controls, Braak III/IV and Braak VI AD specimens analyzed by TaqMan quantitative RT–PCR and normalized to uniformly expressed miR-99a. $^{*}P < 0.05$ and $^{**}P < 0.0001$. $n = 16$ for Braak VI and age-matched controls and $n = 14$ for Braak III/IV specimens. (**C**) Expression of miR-132 (left) and miR-212 (right) in pyramidal neurons laser-captured from CA1 regions of human hippocampi in control and AD specimens. There are five cases in each group of Braak III and Braak VI and four cases in the age-matched controls. Data were normalized to uniformly expressed miR-99a. (**D**) Correlation between miR-132 and miR-212 expression in human control, Braak III/IV and Braak VI specimens analyzed as described for (B). Correlation coefficient $R^2 = 0.5076$ indicates significant correlation. miR-132 and miR-212 levels decline proportionally in Braak III/IV and further in Braak VI. (**E**) Expression of miR-132 and miR-212 in whole-brain sagittal sections (including hippocampus) of double-transgenic APP PS1 mice at 6 months of age. There were four mice per group (wild-type or transgenic) and qRT–PCR data were normalized to uniformly expressed miR-99a.

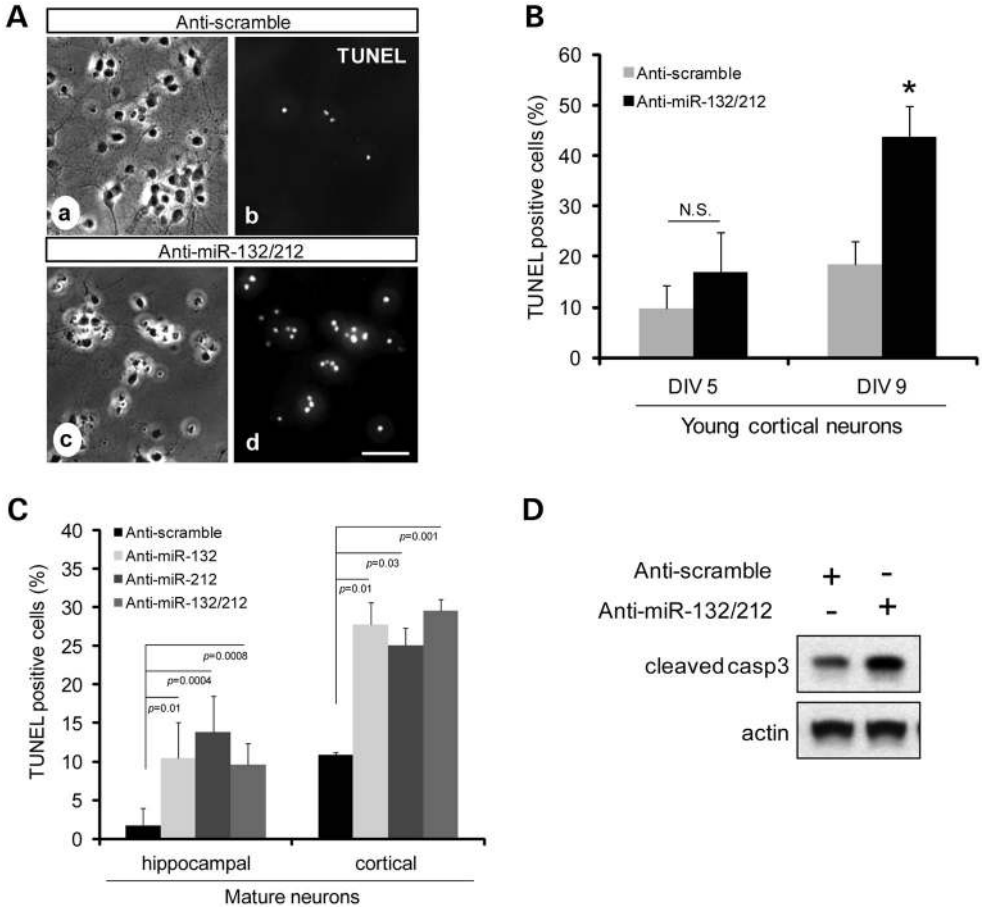

Figure 2. Inhibition of miR-132 and miR-212 in neurons causes apoptosis. (**A**) Representative bright field (a and c) and TUNEL (b and d) images of primary cultured neurons that were transfected with a control inhibitor (anti-scramble, 100 nM) or anti-miR-132/212 (50 nM each) for 7 days. Scale bar = 50 μm. (**B**) Quantification of TUNEL-positive neurons in young neurons transfected with the control inhibitor (anti-scramble) or anti-miR132/212. Young primary cortical neurons were transfected with Lipofectamine 2000 at DIV 2 and collected at DIV 5 and DIV 9 post-transfection. At least 500 neurons were examined in each condition in three independent experiments, $^{*}P < 0.05$. N.S., not significant. (**C**) Quantification of TUNEL-positive neurons in mature neurons transfected with the control inhibitor (anti-scramble) or anti-miR132/212. Mature primary hippocampal or cortical neurons were transfected with NeuroMag at DIV 14 and collected at DIV 28. At least 400 neurons were examined in each condition in three independent experiments. (**D**) A representative western blot shows the expression of cleaved caspase 3 in primary neurons transfected with anti-scramble or anti-miR-132/212 for 2 weeks. Actin serves as a loading control.

hippocampal neurons: there was a 1.7 ± 2.2% basal cell death of neurons transfected with the control inhibitor, and inhibiting miR-132 or miR-212 increased the apoptotic population up to 10.4 ± 4.66 and 13.8 ± 4.74%, respectively (Fig. 2C). Silencing both miR-132 and miR-212 simultaneously did not enhance the apoptotic effect further. At the molecular level, we detected increased levels of cleaved caspase 3 upon miR-132/212 inhibition (Fig. 2D), indicating that inhibition of miR-132/212 initiates neuronal apoptosis through a caspase-dependent pathway.

PTEN and FOXO3a are direct targets of miR-132/212

Having found that miR-132/212 has a role in maintaining neuronal survival, we sought to investigate the mechanism underlying this effect. To identify direct targets that mediate pro-survival function of miR-132/212, we utilized several target-prediction algorithms. Remarkably, PTEN, P300 and FOXO3a, three proteins with established functions in suppressing/antagonizing cell-survival mechanisms, are highly ranked predicted targets for miR-132/212. PTEN is a key negative regulator of PI3K-AKT signaling cascade that is arguably the most important pro-survival pathway in neurons (34). FOXO3a is a pro-apoptotic transcription factor whose activity is suppressed by the AKT signaling (35,36). AKT-phosphorylation of FOXO3a prevents its nuclear translocation and thereby suppresses its activation of pro-apoptotic target genes. P300 acetyltransferase, on the other hand, promotes transcriptional activity of FOXO3a (37). Therefore, it appears that miR-132/212 may regulate several key players that function in the same signaling network by counteracting AKT pro-survival pathway.

P300 protein has been recently validated as a direct target of miR-132 (38). We, therefore, focused on validating two other targets in our subsequent experiments. To show that PTEN and FOXO3a are direct targets of miR-132/212, we employed a dual luciferase reporter system (psiCHECK2). TargetScan (39) and RNAhybrid algorithms (40) predicted three putative binding sites for miR-132 and two sites for miR-212 in the 3′ untranslated region (UTR) of PTEN (site 1: nucleotides/nt 2257–2263; site 2: nt 2874–2881; and site 3: nt 2919–2925). There is a single predicted binding site for miR-132/212 in

FOXO3a 3′ UTR (nt 163–170) (Fig. 3A). psiCHECK2 constructs expressing either 3′ UTR of PTEN or FOXO3a were co-transfected with miR-132 and miR-212 precursors or a corresponding control molecule into PC12 cells. Compared with the control molecule, cotransfection of miR-132/212 with wild-type PTEN 3′ UTR dramatically reduced the reporter gene activity, indicating that miR-132/212 downregulates expression of PTEN (Fig. 3B left panel, PTEN wt $^{*}P < 0.0001$). To identify the binding site of miR-132/212 in PTEN 3′ UTR, we performed a similar luciferase activity assay with mutated reporter constructs. Mutation of site 1, but not 2 or 3, completely abrogated the miR-132/212 regulation of the PTEN 3′ UTR (Fig. 3B left panel, PTEN m1). These data clearly show that miR-132/212 directly binds to nucleotides 2257–2263 of PTEN 3′ UTR and reduces PTEN expression. Similar results were obtained using primary cortical neurons (Fig. 3B right panel, $^{*}P < 0.0001$).

We next showed that miR-132/212 regulates the FOXO3a 3′ UTR, and a mutation within the predicted binding site abolished the binding and regulation [Fig. 3C, $^{*}P < 0.0001$ and (41)]. Consistent with the results obtained with reporter constructs, over-expression of miR-132/212 reduced the levels of PTEN and FOXO3a proteins (Fig. 3D). We conclude that PTEN and FOXO3a are novel, direct targets of miR-132/212 in the neuronal cells.

Activation of P300, PTEN and FOXO3a signaling cascades upon miR-132/212 inhibition

We next investigated the effects of miR-132/212 on the signaling cascade associated with P300, PTEN and FOXO3a targeting. To mimic the reduction of miR-132/212 in AD, we suppressed miR-132/212 in PC12 cells with the specific inhibitors (anti-miR-132 and anti-miR-212). As expected, 2 days after transfection of the inhibitors, we observed a significant increase in the levels of P300, PTEN and FOXO3a proteins (Fig. 4A, $^{*}P < 0.05$). In agreement with the enhanced PTEN expression and activity, we found that phosphorylation of AKT at serine 473 and FOXO3a at serine 253 was largely reduced. Consequently, FOXO3a was more transcriptionally active, since several of its direct downstream mRNA targets, such as BIM, p27 and SOD2, were significantly upregulated upon miR-132/212 inhibition (Fig. 4A). Therefore, in a well-established neural PC12 system, decrease in miR-132/212 leads to the activation of the death-signaling axis, with transcription factor FOXO3a serving as a converging point downstream of P300 and PTEN (Fig. 8).

To confirm these findings in neurons, we performed similar experiments on cultures of primary neurons. We observed a significant increase in P300, PTEN and FOXO3a proteins in young primary neurons, similar to PC12 cells (Fig. 4B left, $^{*}P < 0.05$). Blocking miR-132 or miR-212 individually in mature hippocampal neurons also increased the levels of all three targets, indicating that each miR-132 and miR-212 regulate them in synaptically active neurons (Fig. 4B right). Furthermore, immunostaining experiments revealed that inhibition of miR-132/212 led to nuclear translocation of FOXO3a. There was a 3–4-fold increase of FOXO3a nuclear staining starting from 3 days and lasting up to 2 weeks after a single transfection of anti-miR-132/212 (Fig. 4C right, $^{*}P < 0.05$), indicating a larger population of transcriptionally active FOXO3a. Consistent with this finding, one of the principal pro-apoptotic targets of FOXO3a, BIM, was elevated more than 2-fold (Fig. 4B). Furthermore, significantly increased levels of cleaved caspase 3 indicated that neurons indeed undergo caspase-dependent apoptosis (Fig. 4B). Treating neurons with 10 μM of hydrogen peroxide potentiated the activity of this death axis as we observed an even more prominent increase in P300, PTEN and FOXO3a levels when the apoptotic population was preserved with a pan-caspase inhibitor boc-aspartyl-(Ome)-fluoromethyl-ketone (BAF) (B, Fig. 4D). Therefore, blocking miR-132/212 in neurons initiates a death- signaling cascade that involves P300, PTEN, FOXO3a, BIM and caspase-3.

miR-132/212 loss causes neuronal apoptosis via P300, PTEN and FOXO3a

To test whether the de-repression of P300, PTEN and FOXO3a is directly contributing to the neuronal apoptosis induced by the miR-132/212 inhibitors, we performed a set of rescue experiments. PC12 cells were co-transfected with the miR-132/212 inhibitors and specific small interference RNAs (siRNAs) designed to knock-down either P300, PTEN or FOXO3a, and the effects on cell viability were examined. Effective knock-down on these proteins is shown in Supplementary Material, Figure S4. To enhance the rate of apoptosis via the P300-FOXO3a-BIM axis and mimic AD-related oxidative stress, we treated PC12 cells with hydrogen peroxide (Fig. 4D shows that hydrogen peroxide can effectively enhance this death axis). Hydrogen peroxide treatment is an established experimental system for studying oxidative stress-induced neurodegenerative responses. As shown in Figure 5, miR-132/212 inhibition significantly reduced cell viability of hydrogen peroxide-treated PC12 cells ($13.62 \pm 3.15\%$ cell death; Fig. 5, black bars, $\#P < 0.01$). Knock-down of PTEN, FOXO3a or P300 by the individual cognate siRNAs significantly attenuated anti-miR132/212-induced apoptosis (Fig. 5, light gray bars 3–5, $^{*}P < 0.05$), whereas treatment with a control siRNA had no effect (light gray bars 1–2). Simultaneous knock-down of PTEN, FOXO3a and P300 rescued the anti-miR132/212-induced cell death completely (Fig. 5, dark gray bars, $\#P < 0.01$). These data indicate that miR-132/212 normally functions to maintain neuronal survival by keeping the levels of PTEN, FOXO3a and P300 in check. Significant reduction of miR-132/212 levels, as observed in AD neurons, causes elevation of FOXO3a, activates its pro-apoptotic target genes such as *BIM* and sensitizes the cells to stress signals leading to the neuronal apoptosis.

miR-132/212 protects neurons against hydrogen peroxide-mediated cell death

To further test whether miR-132 and miR-212 protect neurons against apoptotic stimuli, we increased the levels of miR-132 and miR-212 in primary hippocampal neurons by transfecting neurons with miRNA precursor molecules and challenged the cultures with hydrogen peroxide. Treatment of hippocampal neurons with 100 μM hydrogen peroxide for 5 min caused a 40% reduction of cell viability (as observed in WST-1 assay) in 24 h. However, neurons overexpressing miR-132 or miR-212 (pre-miR-132 or -212) were more resistant to this apoptotic

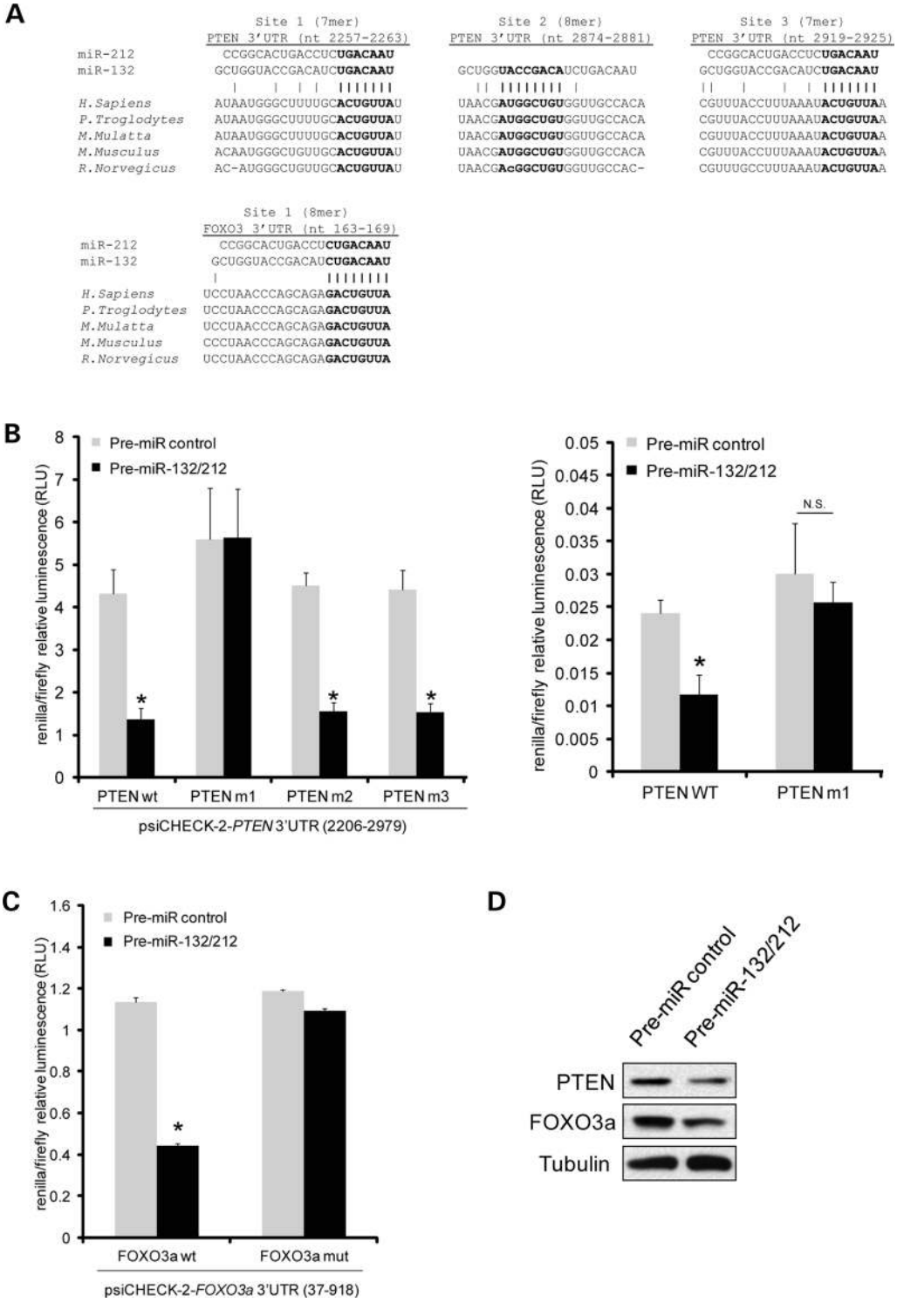

Figure 3. *PTEN* and *FOXO3a* are direct targets of miR-132/212. (**A**) Alignment of predicted miR-132/212 binding sites within the *PTEN* and *FOXO3a* 3′ UTRs is shown for different species. (**B**) Relative activity of wild-type (wt) or mutant (m) psiCHECK-2-*PTEN* 3′ UTR constructs co-transfected with a precursor pre-miRNA control (100 nM) or pre-miR-132/212 (50 nM each) in cultured PC12 cells (left) and primary neurons (right). Error bars represent SEM from three independent transfections; $^{*}P < 0.0001$ and $n = 3$. N.S., not significant. (**C**) Relative activity of wild-type (wt) or mutant (mut) psiCHECK-2-*FOXO3a* 3′ UTR constructs co-transfected with a pre-miRNA control or pre-miR-132/212 in PC12 cells. $^{*}P < 0.0001$ and $n = 3$. Relative activities (that reflect expression levels) in both (B) and (C) are presented as renilla/firefly luminescence (RLU). (**D**) Western immunoblots show the expression of PTEN and FOXO3a in PC12 cells that were transfected with either pre-miRNA-control or pre-miR-132/212 for 2 days. Tubulin serves as a loading control.

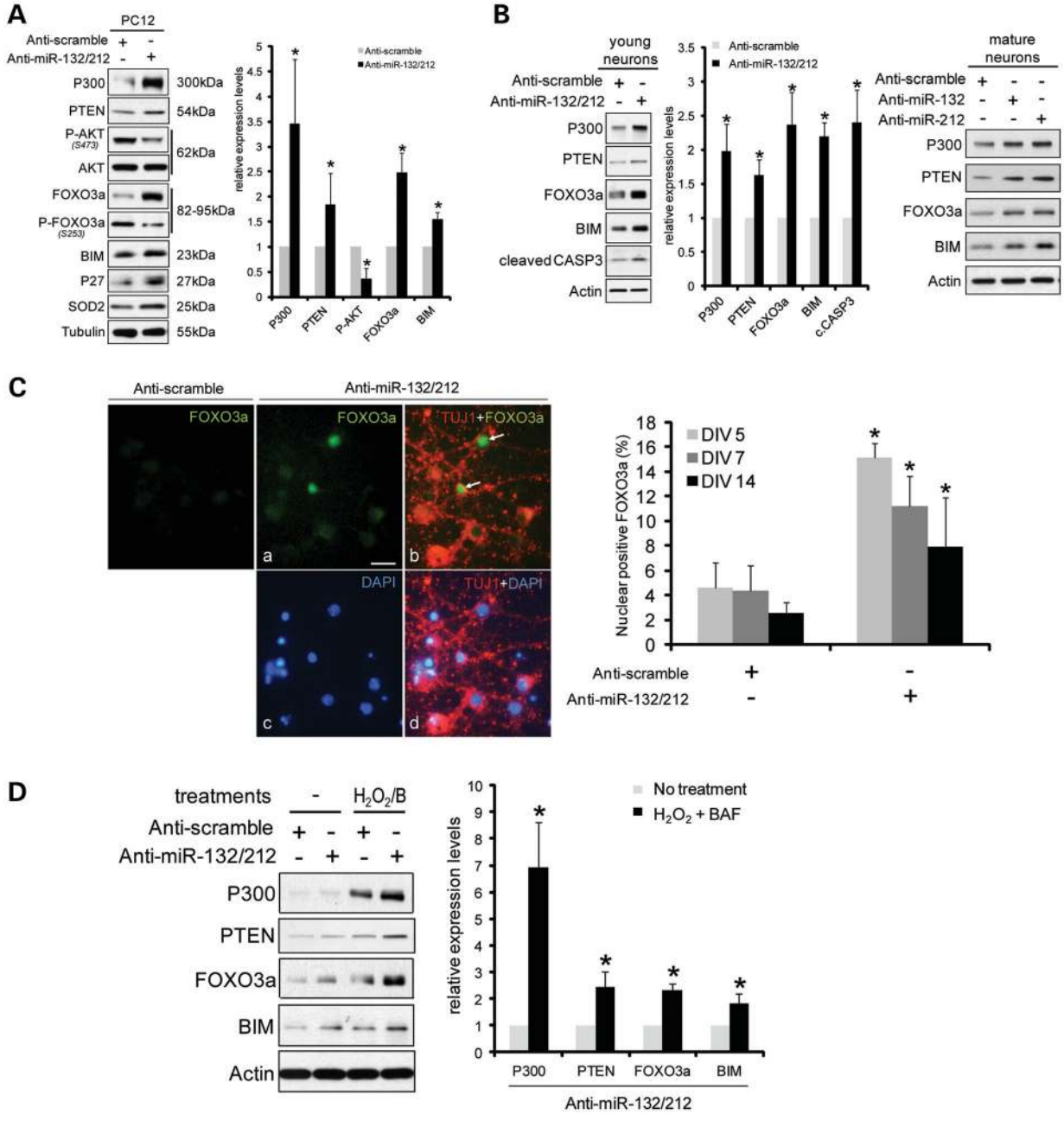

Figure 4. Upregulation of FOXO3a, PTEN and P300 and the associated signaling cascade upon miR-132/212 inhibition. (**A**) PC12 cells were transfected with anti-scramble or anti-miR-132/212 for 2 days and proteins were analyzed with the antibodies indicated in the figure. Blots were scanned and band intensity was quantified using the ImageJ software. Relative expression levels, normalized to tubulin expression, are shown on the right panel. $^*P < 0.05$ and $n = 3$. (**B**) Primary neurons were transfected at DIV 2 (young) or DIV 14 (mature) with anti-scramble control or miR-132/212 inhibitors (individually or together). Proteins were analyzed by western blotting with the antibodies indicated in the diagram. Representative immunoblots are presented and actin-normalized relative expressions are shown graphically. $^*P < 0.05$ and $n = 5$. (**C**) Primary neurons were transfected at DIV2 with the control inhibitor or anti-miR-132/212 and fixed at DIV5, 7 and 14. Neurons were then immunostained with anti-FOXO3a and anti-TUJ1 antibodies (a and b) and mounted with Vetashield supplemented with DAPI (c). The percentage of neurons positive for nuclear FOXO3a was counted and presented on the right. At least 300 neurons were examined in each condition; $^*P < 0.05$ and $n = 3$ with duplicate in each experiment. (**D**) Primary neurons were transfected as in (B), and treated with 10 μM of hydrogen peroxide (H_2O_2) in combination with pan-caspase inhibitor BAF at DIV14 for 15 h. Harvested proteins were analyzed with the antibodies indicated in the diagram. Representative immunoblots are shown on the left and actin-normalized relative expressions are shown graphically on the right (all with anti-miR-132/212 transfection). B, BAF; $^*P < 0.05$ and $n = 5$.

insult: there was a 25–30% increase of survival in cultures transfected with the precursor miRNAs (Fig. 6, middle three bars). Simultaneous overexpression of both miR-132 and miR-212 in the neuronal cultures led to a similar level of protection as that of individual miRNAs (Fig. 6, last two bars). Of note, there was also an increase in cellular metabolism of pre-miR-132/-212-transfected neurons that were not treated with hydrogen peroxide (Fig. 6, first three bars).

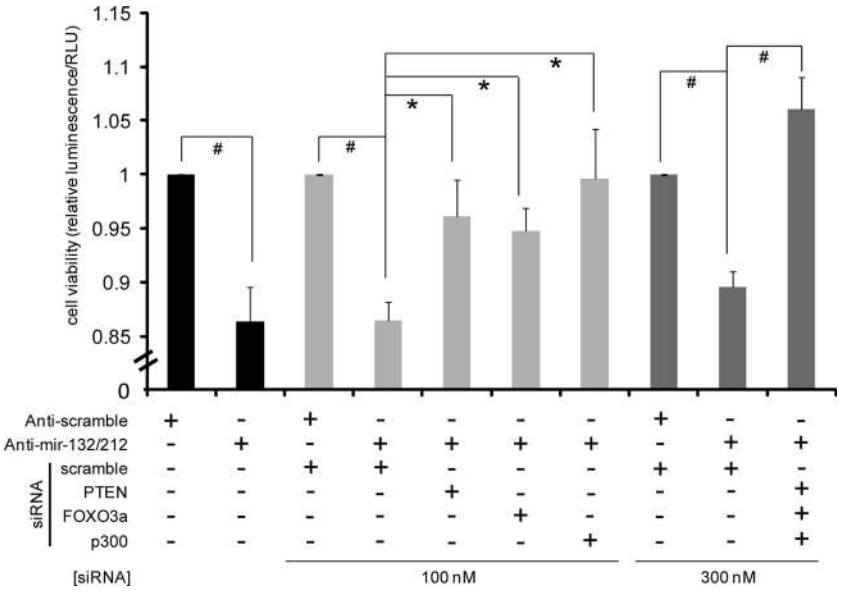

Figure 5. Downregulation of PTEN, FOXO3a and P300 rescues anti-miR-132/212-induced apoptosis. PC12 cells were transfected with the control inhibitor or anti-miR-132/212 (50 nM each) and co-transfected with either control (scramble) siRNA or siRNA cognate to *PTEN*, *FOXO3a* or *P300*, each at 100 nM. In case of simultaneous knockdown of all three miR-132/212 targets, 300 nM of total siRNA was used. The cells were treated with hydrogen peroxide 3 days after transfections. Cell viability was then examined 6–7 h after hydrogen peroxide treatment. $^{*}P < 0.05$ and $\#P < 0.001$, $n = 4$.

miR-132/212 loss is associated with activation of FOXO3a signaling cascades in AD brain tissues

We next attempted to confirm the relevance of our findings to human AD. To this end, we checked the expression of *P300*, *PTEN* and *FOXO3a* mRNAs, and a number of direct transcriptional targets of FOXO3a in the temporal cortex of AD brain specimens (Fig. 7). We used frozen tissues in this experiment since high-fidelity RNA is required for the reliable quantification of mRNA expression in post-mortem specimens. Case information is shown in Supplementary Material, Table S1. Remarkably, expression levels of miR-132/212 targets *P300*, *PTEN* and *FOXO3* were significantly upregulated in AD compared with the age-matched controls (Fig. 7A top panels). Furthermore, mRNA levels of the direct FOXO3a targets such as pro-apoptotic *BIM*, *NOXA* and *PUMA* (BH3 domain-only death proteins), *FASL* (death receptor ligand), *SOD2* and *GADD45a* (stress-response genes) and *P27* (cell-cycle protein) were all significantly increased in Braak VI (Fig. 7A and Supplementary Material, Fig. S5). Moreover, reduced miR-132 expression in human AD brain specimens inversely correlated with the levels of *PTEN* (correlation coefficient $R^2 = 0.4899$), *P300* ($R^2 = 0.4391$), *FOXO3a* ($R^2 = 0.3256$) and *BIM* ($R^2 = 0.4983$) mRNAs (Fig. 7B). We also observed an increased expression of P300, PTEN, FOXO3a and BIM proteins in AD samples compared with their age-matched controls (Fig. 7C). Interestingly, P300, FOXO3a and BIM proteins appeared upregulated in neuronal, Tuj1-normalized, fractions in both gray and white matter of AD specimens, whereas PTEN was found upregulated only in the white matter-enriched portion of the samples. This is in agreement with previous observations, suggesting that PTEN protein is redistributed from cell bodies of normal neurons to intracellular NFTs and degenerative neurites of the damaged neurons in postmortem AD brain tissues (42–45). In conclusion, these results indicate that FOXO3 signaling is activated in AD brains and suggest miR-132/212 as a major regulator of the PTEN/FOXO3 pathway. Figure 8 summarizes the PTEN/P300/FOXO3/BIM signaling cascade activated upon the downregulation of miR-132/212 in AD neurons.

DISCUSSIONS

Aberrant expression of specific miRNA regulators has been reported for a broad range of human disorders, and it often accounts for profound pathological effects associated with disease initiation and/or progression. To date, however, functions of miRNAs dysregulated in AD neurons have not been fully characterized. Here, we identified an miR-132/212 cluster markedly downregulated in CA1 hippocampal neurons isolated from AD brains. This finding is in agreement with the results of several previous studies, including the largest miRNA profiling of AD tissues performed as of today (46,47). Concomitant downregulation of miR-132 and miR-212 levels has been detected as early as at Braak III stage of the disease (usually corresponding to mild cognitive impairment), and becomes highly significant at its end stages (Fig. 1). Reduced levels of miR-132 have also been observed in the brains of human patients suffering from another fatal neurodegenerative disorder, Huntington's disease (48). Whether miR-132 and miR-212 are downregulated not only in neurons but also in glia and other non-neural cells in AD, and if so what impact their reduced levels in these cells have on the disease progression, remains to be further investigated.

Functionally, inhibiting expression of miRNA-132 and miR-212 in cultured primary neurons leads to accumulation of TUNEL-positive neurons and caspase-dependent apoptosis. We identified and experimentally validated two novel direct targets of miR-132/212, PTEN and FOXO3a, both proteins antagonizing AKT survival signaling. Inhibition of miR-132 and

miR-212, individually or simultaneously, de-represses PTEN/FOXO3a signaling and causes apoptosis. Therefore, these two homolog miRNAs share a similar function in the regulation of PTEN/FOXO3a signaling and neural survival. Importantly, knock-down of PTEN, FOXO3a and P300 abrogates miR-132/212-dependent neuronal death. Furthermore, an inverse correlation between the expression levels of miR-132/212 and their targets *PTEN*, *P300* and *FOXO3a* in human brain specimens (Fig. 7B) suggests that miR-132/212 is indeed a key *in vivo* regulator of these proteins. Finally, increased levels of PTEN, P300 and FOXO3a, as well as several key mediators of apoptosis that are directly regulated by FOXO3a (e.g. *BIM*, *PUMA* and *FASL*), are observed in AD specimens (Fig. 7). These results indicate that this pro-apoptotic signaling axis is activated and contributes to the cell death and neurodegeneration in AD. Taken together, we have discovered an miRNA cluster that is deregulated in the disease, and explored its biological function that is linked to the mechanisms leading to neuronal loss in AD.

miRNA-132/212 is a brain-enriched miRNA cluster, and both miRNAs are highly expressed in neurons and neural cells (49–52). Expression of these miRNAs is regulated by neuronal activity, CREB (29,30), neurotrophin (BDNF) (28,51,53) and light (54–57). In AD, it is known that pathologically elevated levels of Aβ lead to synaptic depression (58,59) and destabilize neuronal activity at the circuit and network levels (60). Moreover, a large body of evidence reports that serum or CSF concentrations of BDNF are decreased in AD patients, likely reflecting its intracranial alterations (61–67). Thus, accumulation of Aβ, as well as the reduction of neuronal activity and BDNF levels, might explain the reduced levels of miR-132/212 in AD neurons.

In the nervous system, the key reported function for miR-132/212 is modulation of neuronal morphogenesis, such as regulating dendritic length, spine density and filopodia number through a CREB/p250GAP/RAC1-dependent mechanism (25,26,28,29,68–70). *In vivo*, deletion of miR-132/212 locus in adult hippocampus with a retrovirus expressing Cre recombinase caused a dramatic decrease in dendrite length, arborization and spine density, suggesting that miR-132/212 is required for normal dendritic maturation in adult hippocampal neurons (25). Here, we provide evidence that miR-132/212 has also a role in neuronal survival, and downregulation of these miRNAs induces expression of pro-apoptotic protein Bim, activates caspase-3 and leads to apoptosis in both basal and stress conditions. It has been previously demonstrated that transient activation of mitochondrial pathway of apoptosis in dendrites may lead to local synapse elimination and dendrite pruning without resulting in cell death (71). Therefore, we hypothesize that reduced miR-132/212 levels in AD are likely responsible, in part, for both dendritic deterioration and higher rates of neuronal death, and may lead to both synaptic and neuronal loss observed in the AD brains. How toxic species of Aβ and hyper-phosphorylated tau relate to miR-132/212-dependent neuronal degeneration and death remains to be further investigated.

A number of genes have been previously reported as direct targets for miR-132/212, such as *p250GAP* (28), *MeCP2* (72,73) and *PTBP2* (74). MeCP2 is a major protein implicated in Rett syndrome, and miR-132-mediated dysregulation of PTBP2 might contribute to the abnormal splicing of tau in progressive supranuclear palsy patients and perhaps other tauopathies. Acetyltransferase P300 is also a validated miR-132/212 target (38), which we have found to contribute to miR-132/212-mediated neuronal death. Interestingly, this protein is also involved in tau acetylation and thereby may contribute to pathogenesis of tauopathies (75). Tau is also a predicted direct target for miR-132; however, we were unable to detect regulation of Tau expression by miR-132. Interestingly, miR-132 also regulates expression of acetylcholinesterase (AChE) in immune cells, and inhibition of miR-132 *in vivo* increases AChE activity in the intestine, spleen and serum (76). It would, therefore, be tempting to speculate that miR-132 may also function as an endogenous modulator of AChE in the brain; however, we were unable to detect such activity.

In this study, we provide solid evidence that PTEN and FOXO3a are additional novel targets of miR-132/212, and that decreased levels of miR-132/212 leads to upregulation of both proteins in primary neurons and neural PC12 cells. Of note, both miR-132 and miR-212 directly regulate PTEN and FOXO3a, and inhibition of each miRNA individually caused similar de-repression of these targets in primary neurons. While this manuscript was prepared for submission, a separate report demonstrating that miR-132/212 regulates FOXO3 in cardiomyocytes too was published (41). In our study, FOXO3a was the target most profoundly regulated by miR-132/212 in primary neurons and a converging point in the proposed signaling pathway. The role of this aging-related pro-apoptotic transcription factor activated by reactive oxygen species in AD pathogenesis is just beginning to emerge. Our finding that levels of both FOXO3a and its activator P300 are significantly elevated in Braak VI patients is supported by a microarray analysis of hippocampal gene expression of 9 controls and 22 AD patients [(77) and GSEA from Broad Institute]. Another recent report indicates that FOXO3a might be a common factor elevated in a number of neurodegenerative conditions and suggests it as a possible drug target (78). In neurons, FOXO3a activity is known to increase the production of toxic Aβ species via a ROCK1-dependent mechanism and promotes Aβ-induced neurotoxicity (79). On the other hand, FOXO3a may work downstream of Aβ since insulin-activated AKT protects neuroblastoma cells from Aβ-induced oxidative stress by phosphorylating FOXO3a (80), and FOXO3a is required for $A\beta_{1-42}$-induced microglia activation, proliferation and the subsequent apoptosis (81). Nonetheless, the precise mechanism of interaction between FOXO3a signaling and Aβ toxicity is still poorly explored and it may vary substantially among neurons and other non-neuronal populations involved in AD pathogenesis. Of note, the direct transcriptional target of FOXO3a, BIM, has been shown to be upregulated in AD neurons (82) and is required for Aβ-induced neuronal apoptosis (83). This agrees with the significant BIM upregulation that we observed in AD specimens and upon miR-132/212 inhibition in neurons (Figs 4 and 7). Taken together, it appears that elevated levels of FOXO3a and BIM could lead to the production of Aβ and/or mediate the neurotoxicity of Aβ species. Furthermore, additional FOXO3 transcriptional targets and key regulators of apoptosis, such as FASL and PUMA, are also elevated in Alzheimer's brains and may contribute to neurodegeneration (Fig. 7) (84–86). Further study is required to understand a role of FOXO3 signaling in synaptic impairments as related to the AD pathogenesis.

Three additional miRNAs, miR-22, miR-129 and miR-217, are also bioinformatically predicted to target PTEN, p300 and

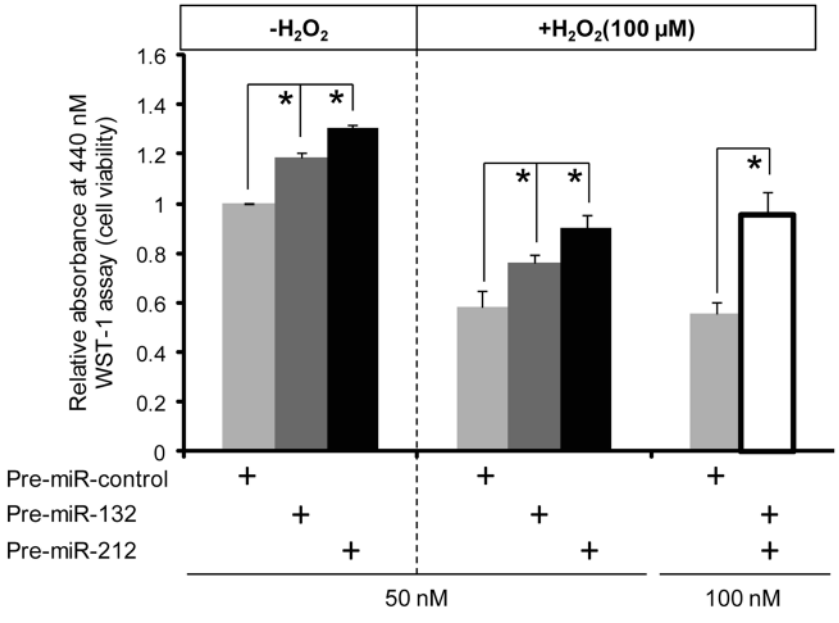

Figure 6. miR-132 and miR-212 overexpression protects primary hippocampal neurons against hydrogen peroxide-mediated cytotoxicity. Young primary hippocampal neurons (at DIV 2) were transfected with control, individual miR-132 or miR-212 mimics, or both (50 nM each). One day after transfection, neurons were challenged with 100 μM of hydrogen peroxide for 5 min at 37°C. Viability of neurons was measured 24 h after H_2O_2 treatment using WST-1 reagent. The viability of cultures transfected with control pre-miRNA was set at 1 and other values were adjusted accordingly. Pre, precursor; $^*P < 0.05$ and $n = 3$ with duplicate in each experiment.

FOXO3a by the TargetScan algorithm. miR-217 is not expressed in neurons, whereas miR-22 appeared to be downregulated in LCM neurons isolated from AD patients (Supplementary Material, Fig. S6), further reinforcing the possibility of miRNA control over this signaling pathway in neurons. Nevertheless, we believe that miR-132 and miR-212 are the main regulators of this pathway as (i) they are the most highly expressed among all five miRNAs (miR-132, miR-212, miR-129, miR-22 and miR-217) in hippocampal neurons (Supplementary Material, Table S2) and therefore their reduced levels in AD would have the major impact on the target genes, and (ii) they are the most highly ranked regulators based on the computational algorithms such as TargetScan (Supplementary Material, Table S2) and PITA. We suggest that upregulation and reactivation of FOXO3 signaling could be one of the central mechanisms regulating neuronal apoptosis upon miR-132/212 repression in AD neurons.

The mechanisms that cause profound degeneration and loss of neurons in AD are not known and the existing information is often controversial and incomplete. The study of miRNA in neurodegenerative disorders is still at its pioneer stage and offers attractive opportunities to gain further insights into mechanism-based regulation of cell death. The short binding seed regions and partial complementarity of miRNAs and their targets could potentially lead to the modulation of multiple members within the same biological network or signaling pathway. Although this idea of miRNA controlling many factors acting along specific signaling axis is very appealing, to the best of our knowledge, only limited examples of such orchestrated regulation have been reported. In this paper, we identified a specific miRNA cluster dysregulated in AD, miR-132/212; explored its role in the disease; and showed that these miRNAs regulate several targets within the same death-causing signaling network. Furthermore, our experiments suggest that replacement of these miRNAs can be neuroprotective. These data not only provide strong evidence that miRNAs are essential molecules in maintaining normal physiology in the nervous system, but also suggest that miRNAs could be important candidates for therapeutic intervention in neurologic impairments.

MATERIALS AND METHODS

Materials

Scramble inhibitor (2′-*O*-MOE PO-Sc, ACATACTCCTTTCTCAGAGTCCA) and antisense inhibitors for miR-132 (2′-*O*-MOE PO-132, CGACCATGGCTGTAGACTGTTA) and miR-212 (2′-*O*-MOE PO-212, GGCCGTGACTGGAGACT GTTA) were obtained from Regulus Therapeutics. The miRNA control molecule, pre-miR-negative control 1 (AM17110) and miR-132 or 212 precursors (AM17100) were from Ambion. SiGENOME control siRNA (D-001220-01-05) was from Thermo scientific. siRNA (the Stealth RNAi) for Pten (PT ENVHS41285), Foxo3a (FOXO3ARSS334413) and P300 (EP300HSS103258) were from Invitrogen. Primary antibodies against AKT (9272), P-AKT (4058S), BIM (2819S), cleaved caspase 3 (9661S), FOXO3a (2497S), P-FOXO3a at serine 253 (9466P), p27 (2552), PTEN (9559) were from Cell Signaling Technology. Primary antibodies against β-ACTIN (ab8229), P300 (ab3164) and SOD2 (ab13534) were from abcam. Primary antibody against α-tubulin (T9026) was from Sigma. Primary antibody against Tuj1 (MMS-435P) was from Covance. Horseradish peroxidase (HRP)-conjugated anti-mouse (7076) and anti-rabbit (7074) secondary antibodies were from Cell Signaling Technology, and Alexa 488-conjugated goat anti-rabbit (A11034) and

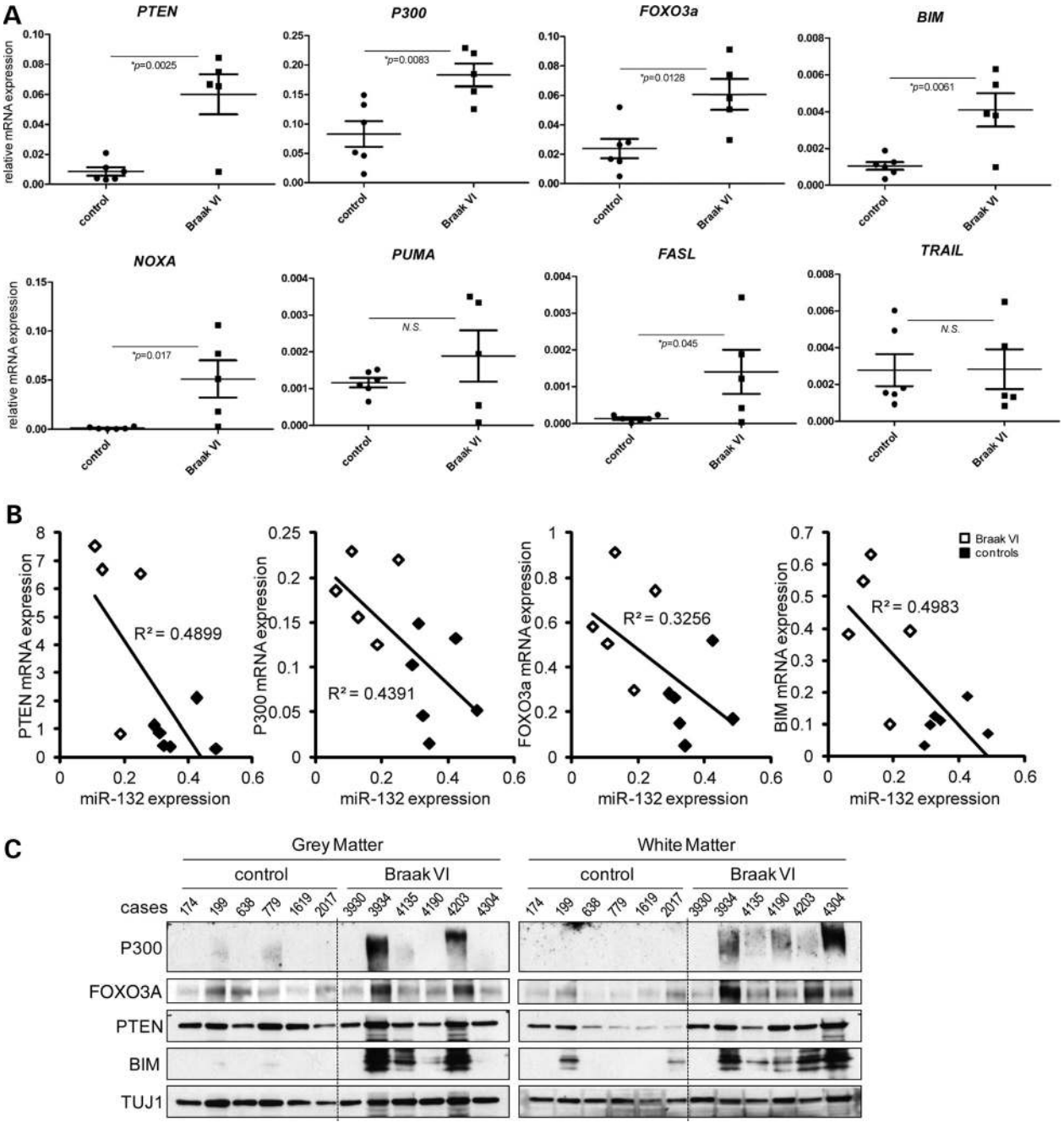

Figure 7. The PTEN/P300/FOXO3a death-signaling axis is activated in the AD brain. (**A**) The mRNA expression of *PTEN*, *P300*, *FOXO3a* and indicated transcriptional targets of FOXO3a in the temporal cortex from AD and control brains were examined by qRT–PCR. The data are normalized to the levels of *18S* rRNA. There is a significant increase in mRNA expression for most of the examined genes in AD Braak VI specimens. Similar results were obtained with normalization to actin mRNA levels. **P*-values are indicated in the graphs and N.S. means not significant. There are five cases analyzed in the Braak VI group and six cases in the age-matched controls. (**B**) The expression correlation between the levels of miR-132 and its mRNA targets. mRNA levels were quantified as indicated in (A). Correlation plots show that expression of miR-132 inversely correlates with its target genes *PTEN*, *P300*, *FOXO3a* and downstream mediator of apoptosis *BIM*. (**C**) Frozen human samples of AD Braak VI and age-matched controls from the cerebral temporal lobe regions were dissected into gray- and white matter-enriched portions. The samples were homogenized and proteins analyzed with the antibodies indicated in the diagram. TUJ1 serves as a maker for neuronal input and total protein loading.

Alexa 594-conjugated anti-mouse (A11032) secondary antibodies were from Molecular Probes. Broad caspase inhibitor BAF (IMI-2311-5) was obtained from Imgenex, and hydrogen peroxide (216763) was from Sigma.

Frozen and fixed human post-mortem brain specimens were obtained from the Harvard Brain Tissue Resource Center and New York Brain Bank at Columbia University and used in accordance with the policies of Brigham and Women's Hospital's institutional review board. Formaldehyde-fixed, paraffin-embedded sagittal brain sections of APP PS1 transgenic mice and littermate controls were utilized for miRNA analysis.

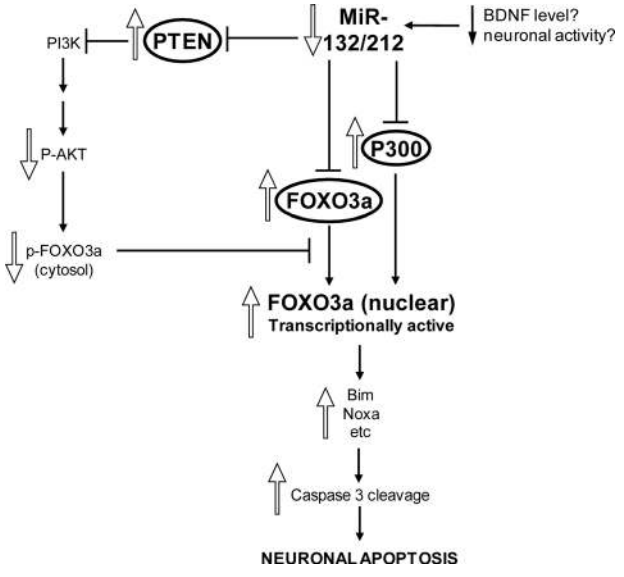

Figure 8. The proposed model of miR-132/212-mediated neuronal apoptosis. miR-132/212 is regulated by BDNF and neuronal activity, which are significantly reduced in AD (please see DISCUSSION). The diminished levels of miR-132/212 lead to de-repression of PTEN, P300 and FOXO3a, and thus activate a signaling cascade that converges at transcription factor FOXO3a. FOXO3a translocates to nucleus and transcribes pro-apoptotic genes such as BIM and NOXA. Caspase-3 is cleaved, causing apoptotic cell death in neurons.

Cell cultures

Primary cerebrocortical neurons were prepared from either an embryonic (E) day 16 imprinting control region mouse or an E18 Spargue–Dawley rat. Cerebral cortices were isolated from embryos and freed from meninges. Cortical tissues were first digested with 0.25% trypsin in Hank's balanced salt solution (HBSS) for 15 min at 37°C. Digested tissues were then washed three times with HBSS and triturated with fire-polished glass pipettes until single cells were obtained. Cell suspension was then filtered through a 70 and a 40 μm cell strainer and subjected to a spin at 1000*g* for a few minutes. Supernatant was removed and cell pellet was resuspended with 10 ml of HBSS. Cell density was then determined with a hemocytometer and cells were seeded at different densities according to the experimental design and need. We used Dulbecco's modified Eagle's media (DMEM) supplemented with 10% FBS for the initial plating, and the medium was changed to Neurobasal supplemented with 1× B27 (Invitrogen) in 3 h. Half medium was changed every 3 days. PC12 cells were maintained in DMEM supplemented with 10% horse serum and 5% FBS.

Transfection of PC12 cells and young (day *in vitro* 2) primary neurons

Transfections of siRNA and miRNA precursors or inhibitors were performed with Lipofectamine 2000 (Gibco) according to the manufacturer's instructions. We used miRNA precursors or inhibitors at 50 nM and siRNA at 100 nM final concentration. Primary neurons were transfected at day *in vitro* (DIV) 2 for 2 h, the medium was replaced completely to avoid toxicity and the cells were analyzed by various assays after 5–21 days.

Transfection of mature (DIV 14–21) primary neurons

Transfections of the oligonucleotide inhibitors into mature primary neurons have been carried out using the magnetism-based technology developed by the OZ Biosciences (NeuroMag). Oligonucleotides at 50 nM were mixed with nanoparticles (200× dilution) in the Neurobasal medium at room temperature for 15 min. Transfection complex was then added to the cells and the culture plate placed on a magnetic plate (OZ Biosciences) at room temperature for additional 15 min. The cultures were incubated with the transfection mixture overnight in a standard culture incubator. Half of the medium was replaced on the next morning, and the remaining medium at later time points.

Extraction of total RNA

To extract total RNA from frozen biopsy samples, we used the TRIZOL reagent (Invitrogen) according to the manufacturer's instructions. Equal portions of white and gray matter from the temporal lobe were dissected and homogenized. All RNA samples were analyzed with Nanodrop to ensure high purity and quality. From formalin-fixed and paraffin-embedded human and mouse tissues, RNA was isolated using Recover All™ Total Nucleic Acid Isolation Kit according to the provided instructions (Ambion).

Laser-capture microdissection of hippocampal neurons from CA1 regions and RNA isolation

To quantify expression changes in individual CA1 hippocampal neurons, frozen tissues from the medial temporal lobe were obtained from Control, Braak III and Braak VI AD subjects (Supplementary Material, Fig. S1C). Frozen human postmortem brain specimens were obtained from the Massachusetts Alzheimer's Disease Research Center (MADRC) and used in accordance with the policies of the Massachusetts General Hospital's institutional review board.

For cytoarchitectural visualization of the CA1 region of the hippocampus, each hippocampus was grossly dissected, blocked and oriented on the cryotome stage. Ten-micrometer thin cryo-sections were mounted on microscopy slides (Gold Seal Rite-On Micro Slides, Thermo Scientific, 12518-101) and processed for LCM within 24 h of tissue sectioning.

Each section was lightly fixed in 70% ethanol for 30 s. The sections were then rinsed with RNAse-free distilled water and incubated in the Arcturus histogene staining solution (Applied Biosystems, KIT0415) for 1 min followed by dehydration in increasingly concentrated ethanol 75–100% into xylene before LCM. All incubations and washes were carried out at room temperature. Owing to the neurodegenerative status of hippocampi, the number of CA1 neurons available for capturing varied greatly among cases. Approximately 2000 CA1 neurons were obtained from 5–8 sections from each control subject, 10–15 sections from each Braak and Braak III subject and 15–25 sections from each Braak VI subject.

RNA was isolated using the Arcturus picopure RNA isolation system, with modifications allowing purification of miRNAs (Applied Biosystems, KIT0204). Polyethylene LCM collecting caps were incubated at 42°C for 30 min in 20 μl of the kit's GITC-containing extraction buffer, centrifuged briefly to

collect the extracted solution and then frozen at −80°C. Prior to purification on the kit's picopure RNA columns, samples were thawed, pooled and mixed with 100% ethanol in a 2:3 volume ratio to increase ethanol concentration and therefore allow for the binding of miRNAs. Samples were placed on the columns and centrifuged to bind RNA to the column, and the procedure was repeated to ensure the binding. Genomic DNA was removed by RNase-free DNase (Qiagen, 79254) digestion on the columns. Total cellular RNA was eluted from the columns in a two-step process, each with 7.5 μl of elution buffer, and stored at −80°C until further analysis.

miRNA expression

We used TaqMan miRNA reverse transcription reagents (Applied Biosystems, 4366596) and miR 5× RT primers (Applied Biosystems, hsa-miR-132/ RT457; hsa-miR-212/ RT515 and hsa-miR-99a/RT435) for reverse transcription. Five nanograms of RNA was used for the initial input. To investigate expression of specific miRNA, we used TaqMan Universal PCR Master Mix (Applied Biosystems, 4324018) with miRNA real-time PCR primers (Applied Biosystems, hsa-miR-132/ TM457; hsa-miR-212/TM515 and hsa-miR-99a/TM435). Real-time reactions were carried out by the ViiA-7 or 7500 Fast System (Applied Biosystems). Threshold cycles (Cts) were generated using the automatic option and the relative expressions were presented as $2^{-\mathrm{deltaCt}}$.

Messenger RNA expression

We transcribed 1 μg of RNA with TaqMan Reverse Transcription Reagents (Applied Biosystems, N808–0234) and investigated gene expression levels using syber green-based chemistry (Applied Biosystems SYBR Green PCR Master Mix, 4309155). Please refer to Supplementary Material, Table S3 for real-time PCR primer sequences. The primers have been checked for primer-dimer formation and used at final concentrations ranging from 40 to 200 nM.

Validation of miR-132/212 targets

We validated targets of miR-132/212 using psiCHECK2 constructs (Promega, C8021). Nucleotides 2206–2979 of *PTEN* 3′ UTR, or 37–918 of *FOXO3a* 3′ UTR, was cloned into psiCHECK2 downstream of *renilla* luciferase, using *Xho*I and *Not*I. Primers used for cloning *PTEN* 3′ UTR were (all 5′ to 3′): forward CCGCTCGAGTGTAACATGGAGGGCCAGGTC and reverse ATAAGAATGCGGCCGCAAGCCCCCACTTTAGTGCACA. Primers used for cloning *FOXO3a* 3′ UTR were: forward CGTCTCGAGCCCTCAAACTGACACAAGACCTAC and reverse CGTAGCGGCCGCAATGAGTGGAGAGCTGAGCTG. Mutations were introduced into the wild-type constructs, using QuikChange Multi Site-Directed Mutagenesis Kit (Stratagene, 200514). Primers used to mutate *PTEN* site 1 were: forward ATGGGCTTTTGCACCAGGATTATTTTTCCTTTGG and reverse CCAAAGGAAAAATAATCCTGGTGCAAAAGCCCAT. *PTEN* site 2: forward GTTCATAACGATAATTGTGGTTGCCACAAAGTGC and reverse GCACTTTGTGGCAACCACAATTATCGTTATGAAC. *PTEN* site 3: forward ACCTTTAAATACCAGGAATGTGTCATGCATGC and reverse GCATGCATGACACATTCCTGGTATTTAAAGGT. *FOXO3a* site 1: forward CCATTTTCCTAACCCAGCAGAGAGCTCTAATGGCCCCTTACCCT and reverse AGGGTAAGGGGCCATTAGAGCTCTCTGCTGGGTTAGGAAAATGG. Two hundred nanograms of psiCHECK2 construct, together with miR precursors at 50 nM final concentration, was transfected into PC12 cells (96 wells) with Lipofectamine 2000. To validate targets using primary neurons, 1 μg of psiCHECK2 construct was used in each of 24 wells. Two days after transfection, luciferase luminescence was revealed with Dual-Glo Luciferase Assay System (Promega, E2920) and detected with Infinite F200 plate reader (TECAN). Renilla luminescence was normalized with that of firefly and the signals are presented as renilla/firefly relative luminescence.

TUNEL assay

TUNEL assay was employed to detect DNA strand breaks and used to quantify cells that were undergoing apoptosis. We used *In Situ* Cell Death Detection Kit, TMR red (Roche, 12156792910) to reveal apoptotic cells. In brief, cells were first fixed with 4% paraformaldehyde for 1 h at room temperature and then permeabilized with 0.1% Triton X-100 in 0.1% sodium citrate for 2 min on ice. The cells were further incubated with TUNEL reaction mixture for 1 h at 37°C, mounted with VECTASHIELD (Vector) supplemented with DAPI and analyzed by fluorescence microscopy with an excitation wavelength in the range of 520–560 nm (green) and detection in the range of 570–620 nm (red).

Cell viability assays

For the rescue experiment on PC12 cells, we examined cell viability with a luciferase/ATP-based assay from Promega (the CellTiter-Glo Luminescent Cell Viability Assay, G7571) according to the manufacturer's instructions. Cells were incubated with CellTiter-Glo reagent for 10 min at room temperature and luciferase signals were measured with a plate reader Infinite F200 (TECAN). To measure cell viability of hydrogen peroxide-treated primary hippocampal neurons, we used WST-1 reagent (Roche, 05015944001). Briefly, cells were incubated with the WST-1 reagent at 1:10 dilution at 37°C for 1 h. Medium was then aliquoted in a 96-well plate and absorbance was measured at 440 nM using a plate reader. The absorbance directly correlates with the number of viable cells/mitochondria in a fixed given area.

Western blot analysis

Cells were rinsed with cold PBS and lysed in an appropriate volume of lysis buffer. Protein concentrations were measured with Micro Bicinchoninic Acid (BCA) Protein Assay Kit (Pierce, 23235) according to the manufacturer's instructions. Appropriate volumes of protein lysates were then mixed with 6× SDS gel-loading buffer (Boston Bioproducts), boiled for 5 min and resolved in 8–16% gradient polyacrylamide gels (Invitrogen). Proteins were subsequently transferred onto a polyvinylidene fluoride membrane (0.45 μm, Thermo Scientific) and the membrane was blocked with 5% non-fat milk in Tris-

buffered saline with Tween-20 (TBS-T) for 1 h. Blots were then incubated with appropriately diluted primary antibody overnight at 4°C. Blots were washed with TBS-T a few times next day, and HRP-conjugated secondary antibodies were added for 1 h. Finally, after a few washes, blots were developed with enhanced chemiluminescence solutions (GE Healthcare Amersham, RPN2209) and exposed onto HyBlot CL (Denville Scientific).

Immunocytochemistry

Cells were first fixed with 4% paraformaldehyde in PBS at 4°C for 20 min and permeabilized with 0.3% Trion X-100 for 5 min. Cells were then blocked with 5% non-fat milk for 1 h and incubated with appropriately diluted primary antibody at 4°C overnight. After primary antibody incubation, cells were washed three times with PBS and subsequently incubated with fluorescence-conjugated secondary antibodies at room temperature for 1 h in the dark. Cells were finally washed three times with PBS and mounted in VECTASHIELD® (Vector) and analyzed by fluorescent microscopy.

Statistical analysis

We used the unpaired, two-tailed Student's *t*-test for comparison between two samples. We considered the difference between comparisons to be significant when $P < 0.05$ for all the statistical analysis. All values were presented as mean ± SEM.

SUPPLEMENTARY MATERIAL

Supplementary Material is available at *HMG* online.

ACKNOWLEDGEMENTS

We would like to acknowledge the Harvard NeuroDiscovery Center for supporting this project via the Advanced Tissue Resource Center, Jeffrey L. Frost for technical assistance and Athul Mohan for helping with the extraction of RNA from formalin-fixed, paraffin-embedded brain sections.

Conflict of Interest statement. None declared.

FUNDING

This work was supported by a grant from the Alzheimer's Association (NIRG-09-132844).

REFERENCES

1. Turner, R.S. (2006) Alzheimer's disease. *Semin. Neurol.*, **26**, 499–506.
2. Castro, R.E., Santos, M.M., Gloria, P.M., Ribeiro, C.J., Ferreira, D.M., Xavier, J.M., Moreira, R. and Rodrigues, C.M. (2010) Cell death targets and potential modulators in Alzheimer's disease. *Curr. Pharm. Des.*, **16**, 2851–2864.
3. Krichevsky, A.M., King, K.S., Donahue, C.P., Khrapko, K. and Kosik, K.S. (2003) A microRNA array reveals extensive regulation of microRNAs during brain development. *RNA*, **9**, 1274–1281.
4. Sempere, L.F., Freemantle, S., Pitha-Rowe, I., Moss, E., Dmitrovsky, E. and Ambros, V. (2004) Expression profiling of mammalian microRNAs uncovers a subset of brain-expressed microRNAs with possible roles in murine and human neuronal differentiation. *Genome Biol.*, **5**, R13.
5. Berezikov, E., Thuemmler, F., van Laake, L.W., Kondova, I., Bontrop, R., Cuppen, E. and Plasterk, R.H. (2006) Diversity of microRNAs in human and chimpanzee brain. *Nat. Genet.*, **38**, 1375–1377.
6. Landgraf, P., Rusu, M., Sheridan, R., Sewer, A., Iovino, N., Aravin, A., Pfeffer, S., Rice, A., Kamphorst, A.O., Landthaler, M. *et al.* (2007) A mammalian microRNA expression atlas based on small RNA library sequencing. *Cell*, **129**, 1401–1414.
7. Ambros, V. (2004) The functions of animal microRNAs. *Nature*, **431**, 350–355.
8. Djuranovic, S., Nahvi, A. and Green, R. (2011) A parsimonious model for gene regulation by miRNAs. *Science*, **331**, 550–553.
9. Liu, N.K. and Xu, X.M. (2011) MicroRNA in central nervous system trauma and degenerative disorders. *Physiol. Genomics*, **43**, 571–580.
10. Zovoilis, A., Agbemenyah, H.Y., Agis-Balboa, R.C., Stilling, R.M., Edbauer, D., Rao, P., Farinelli, L., Delalle, I., Schmitt, A., Falkai, P. *et al.* (2011) microRNA-34c is a novel target to treat dementias. *EMBO J.*, **30**, 4299–4308.
11. Patel, N., Hoang, D., Miller, N., Ansaloni, S., Huang, Q., Rogers, J.T., Lee, J.C. and Saunders, A.J. (2008) MicroRNAs can regulate human APP levels. *Mol. Neurodegener.*, **3**, 10.
12. Hebert, S.S., Horre, K., Nicolai, L., Bergmans, B., Papadopoulou, A.S., Delacourte, A. and De Strooper, B. (2009) MicroRNA regulation of Alzheimer's amyloid precursor protein expression. *Neurobiol. Dis.*, **33**, 422–428.
13. Vilardo, E., Barbato, C., Ciotti, M., Cogoni, C. and Ruberti, F. (2010) MicroRNA-101 regulates amyloid precursor protein expression in hippocampal neurons. *J. Biol. Chem.*, **285**, 18344–18351.
14. Liu, W., Liu, C., Zhu, J., Shu, P., Yin, B., Gong, Y., Qiang, B., Yuan, J. and Peng, X. (2010) MicroRNA-16 targets amyloid precursor protein to potentially modulate Alzheimer's-associated pathogenesis in SAMP8 mice. *Neurobiol. Aging*, **33**, 522–534.
15. Long, J.M. and Lahiri, D.K. (2011) MicroRNA-101 downregulates Alzheimer's amyloid-beta precursor protein levels in human cell cultures and is differentially expressed. *Biochem. Biophys. Res. Commun.*, **404**, 889–895.
16. Long, J.M., Ray, B. and Lahiri, D.K. (2012) MicroRNA-153 physiologically inhibits expression of amyloid-beta precursor protein in cultured human fetal brain cells and is dysregulated in a subset of Alzheimer disease patients. *J. Biol. Chem.*, **287**, 31298–31310.
17. Liang, C., Zhu, H., Xu, Y., Huang, L., Ma, C., Deng, W., Liu, Y. and Qin, C. (2012) MicroRNA-153 negatively regulates the expression of amyloid precursor protein and amyloid precursor-like protein 2. *Brain Res.*, **1455**, 103–113.
18. Smith, P., Al Hashimi, A., Girard, J., Delay, C. and Hebert, S.S. (2011) In vivo regulation of amyloid precursor protein neuronal splicing by microRNAs. *J. Neurochem.*, **116**, 240–247.
19. Wang, W.X., Rajeev, B.W., Stromberg, A.J., Ren, N., Tang, G., Huang, Q., Rigoutsos, I. and Nelson, P.T. (2008) The expression of microRNA miR-107 decreases early in Alzheimer's disease and may accelerate disease progression through regulation of beta-site amyloid precursor protein-cleaving enzyme 1. *J. Neurosci.*, **28**, 1213–1223.
20. Boissonneault, V., Plante, I., Rivest, S. and Provost, P. (2009) MicroRNA-298 and microRNA-328 regulate expression of mouse beta-amyloid precursor protein-converting enzyme 1. *J. Biol. Chem.*, **284**, 1971–1981.
21. Hebert, S.S., Horre, K., Nicolai, L., Papadopoulou, A.S., Mandemakers, W., Silahtaroglu, A.N., Kauppinen, S., Delacourte, A. and De Strooper, B. (2008) Loss of microRNA cluster miR-29a/b-1 in sporadic Alzheimer's disease correlates with increased BACE1/beta-secretase expression. *Proc. Natl Acad. Sci. USA*, **105**, 6415–6420.
22. Zhu, H.C., Wang, L.M., Wang, M., Song, B., Tan, S., Teng, J.F. and Duan, D.X. (2012) MicroRNA-195 downregulates Alzheimer's disease amyloid-beta production by targeting BACE1. *Brain Res. Bull.*, **88**, 596–601.
23. Fang, M., Wang, J., Zhang, X., Geng, Y., Hu, Z., Rudd, J.A., Ling, S., Chen, W. and Han, S. (2012) The miR-124 regulates the expression of BACE1/beta-secretase correlated with cell death in Alzheimer's disease. *Toxicol. Lett.*, **209**, 94–105.
24. Wang, X., Liu, P., Zhu, H., Xu, Y., Ma, C., Dai, X., Huang, L., Liu, Y., Zhang, L. and Qin, C. (2009) miR-34a, a microRNA up-regulated in a double transgenic mouse model of Alzheimer's disease, inhibits bcl2 translation. *Brain Res. Bull.*, **80**, 268–273.

25. Magill, S.T., Cambronne, X.A., Luikart, B.W., Lioy, D.T., Leighton, B.H., Westbrook, G.L., Mandel, G. and Goodman, R.H. (2010) microRNA-132 regulates dendritic growth and arborization of newborn neurons in the adult hippocampus. *Proc. Natl Acad. Sci. USA*, **107**, 20382–20387.
26. Edbauer, D., Neilson, J.R., Foster, K.A., Wang, C.F., Seeburg, D.P., Batterton, M.N., Tada, T., Dolan, B.M., Sharp, P.A. and Sheng, M. (2010) Regulation of synaptic structure and function by FMRP-associated microRNAs miR-125b and miR-132. *Neuron*, **65**, 373–384.
27. Jankowsky, J.L., Younkin, L.H., Gonzales, V., Fadale, D.J., Slunt, H.H., Lester, H.A., Younkin, S.G. and Borchelt, D.R. (2007) Rodent A beta modulates the solubility and distribution of amyloid deposits in transgenic mice. *J. Biol. Chem.*, **282**, 22707–22720.
28. Vo, N., Klein, M.E., Varlamova, O., Keller, D.M., Yamamoto, T., Goodman, R.H. and Impey, S. (2005) A cAMP-response element binding protein-induced microRNA regulates neuronal morphogenesis. *Proc. Natl Acad. Sci. USA*, **102**, 16426–16431.
29. Wayman, G.A., Davare, M., Ando, H., Fortin, D., Varlamova, O., Cheng, H.Y., Marks, D., Obrietan, K., Soderling, T.R., Goodman, R.H. *et al.* (2008) An activity-regulated microRNA controls dendritic plasticity by down-regulating p250GAP. *Proc. Natl Acad. Sci. USA*, **105**, 9093–9098.
30. Nudelman, A.S., DiRocco, D.P., Lambert, T.J., Garelick, M.G., Le, J., Nathanson, N.M. and Storm, D.R. (2010) Neuronal activity rapidly induces transcription of the CREB-regulated microRNA-132, in vivo. *Hippocampus*, **20**, 492–498.
31. Scott, H.L., Tamagnini, F., Narduzzo, K.E., Howarth, J.L., Lee, Y.B., Wong, L.F., Brown, M.W., Warburton, E.C., Bashir, Z.I. and Uney, J.B. (2012) MicroRNA-132 regulates recognition memory and synaptic plasticity in the perirhinal cortex. *Eur. J. Neurosci.*, **36**, 2941–2948.
32. Davis, S., Lollo, B., Freier, S. and Esau, C. (2006) Improved targeting of miRNA with antisense oligonucleotides. *Nucleic Acids Res.*, **34**, 2294–2304.
33. Gabriely, G., Wurdinger, T., Kesari, S., Esau, C.C., Burchard, J., Linsley, P.S. and Krichevsky, A.M. (2008) MicroRNA 21 promotes glioma invasion by targeting matrix metalloproteinase regulators. *Mol. Cell. Biol.*, **28**, 5369–5380.
34. Stambolic, V., Suzuki, A., de la Pompa, J.L., Brothers, G.M., Mirtsos, C., Sasaki, T., Ruland, J., Penninger, J.M., Siderovski, D.P. and Mak, T.W. (1998) Negative regulation of PKB/Akt-dependent cell survival by the tumor suppressor PTEN. *Cell*, **95**, 29–39.
35. Brunet, A., Bonni, A., Zigmond, M.J., Lin, M.Z., Juo, P., Hu, L.S., Anderson, M.J., Arden, K.C., Blenis, J. and Greenberg, M.E. (1999) Akt promotes cell survival by phosphorylating and inhibiting a Forkhead transcription factor. *Cell*, **96**, 857–868.
36. Yang, J.Y. and Hung, M.C. (2009) A new fork for clinical application: targeting forkhead transcription factors in cancer. *Clin. Cancer Res.*, **15**, 752–757.
37. Motta, M.C., Divecha, N., Lemieux, M., Kamel, C., Chen, D., Gu, W., Bultsma, Y., McBurney, M. and Guarente, L. (2004) Mammalian SIRT1 represses forkhead transcription factors. *Cell*, **116**, 551–563.
38. Lagos, D., Pollara, G., Henderson, S., Gratrix, F., Fabani, M., Milne, R.S., Gotch, F. and Boshoff, C. (2010) miR-132 regulates antiviral innate immunity through suppression of the p300 transcriptional co-activator. *Nat. Cell Biol.*, **12**, 513–519.
39. Grimson, A., Farh, K.K., Johnston, W.K., Garrett-Engele, P., Lim, L.P. and Bartel, D.P. (2007) MicroRNA targeting specificity in mammals: determinants beyond seed pairing. *Mol. Cell*, **27**, 91–105.
40. Rehmsmeier, M., Steffen, P., Hochsmann, M. and Giegerich, R. (2004) Fast and effective prediction of microRNA/target duplexes. *RNA*, **10**, 1507–1517.
41. Ucar, A., Gupta, S.K., Fiedler, J., Erikci, E., Kardasinski, M., Batkai, S., Dangwal, S., Kumarswamy, R., Bang, C., Holzmann, A. *et al.*. (2012) The miRNA-212/132 family regulates both cardiac hypertrophy and cardiomyocyte autophagy. *Nat. Commun.*, **3**, 1078.
42. Sonoda, Y., Mukai, H., Matsuo, K., Takahashi, M., Ono, Y., Maeda, K., Akiyama, H. and Kawamata, T. (2010) Accumulation of tumor-suppressor PTEN in Alzheimer neurofibrillary tangles. *Neurosci. Lett.*, **471**, 20–24.
43. Zhang, X., Li, F., Bulloj, A., Zhang, Y.W., Tong, G., Zhang, Z., Liao, F.F. and Xu, H. (2006) Tumor-suppressor PTEN affects tau phosphorylation, aggregation, and binding to microtubules. *FASEB J.*, **20**, 1272–1274.
44. Rickle, A., Bogdanovic, N., Volkmann, I., Zhou, X., Pei, J.J., Winblad, B. and Cowburn, R.F. (2006) PTEN levels in Alzheimer's disease medial temporal cortex. *Neurochem. Int.*, **48**, 114–123.
45. Griffin, R.J., Moloney, A., Kelliher, M., Johnston, J.A., Ravid, R., Dockery, P., O'Connor, R. and O'Neill, C. (2005) Activation of Akt/PKB, increased phosphorylation of Akt substrates and loss and altered distribution of Akt and PTEN are features of Alzheimer's disease pathology. *J. Neurochem.*, **93**, 105–117.
46. Cogswell, J.P., Ward, J., Taylor, I.A., Waters, M., Shi, Y., Cannon, B., Kelnar, K., Kemppainen, J., Brown, D., Chen, C. *et al.* (2008) Identification of miRNA changes in Alzheimer's disease brain and CSF yields putative biomarkers and insights into disease pathways. *J. Alzheimers Dis.*, **14**, 27–41.
47. Wang, W.X., Huang, Q., Hu, Y., Stromberg, A.J. and Nelson, P.T. (2011) Patterns of microRNA expression in normal and early Alzheimer's disease human temporal cortex: white matter versus gray matter. *Acta Neuropathol.*, **121**, 193–205.
48. Johnson, R., Zuccato, C., Belyaev, N.D., Guest, D.J., Cattaneo, E. and Buckley, N.J. (2008) A microRNA-based gene dysregulation pathway in Huntington's disease. *Neurobiol. Dis.*, **29**, 438–445.
49. Olsen, L., Klausen, M., Helboe, L., Nielsen, F.C. and Werge, T. (2009) MicroRNAs show mutually exclusive expression patterns in the brain of adult male rats. *PLoS One*, **4**, e7225.
50. Hollander, J.A., Im, H.I., Amelio, A.L., Kocerha, J., Bali, P., Lu, Q., Willoughby, D., Wahlestedt, C., Conkright, M.D. and Kenny, P.J. (2010) Striatal microRNA controls cocaine intake through CREB signalling. *Nature*, **466**, 197–202.
51. Remenyi, J., Hunter, C.J., Cole, C., Ando, H., Impey, S., Monk, C.E., Martin, K.J., Barton, G.J., Hutvagner, G. and Arthur, J.S. (2010) Regulation of the miR-212/132 locus by MSK1 and CREB in response to neurotrophins. *Biochem. J.*, **428**, 281–291.
52. Somel, M., Guo, S., Fu, N., Yan, Z., Hu, H.Y., Xu, Y., Yuan, Y., Ning, Z., Hu, Y., Menzel, C. *et al.* (2010) MicroRNA, mRNA, and protein expression link development and aging in human and macaque brain. *Genome Res.*, **20**, 1207–1218.
53. Kawashima, H., Numakawa, T., Kumamaru, E., Adachi, N., Mizuno, H., Ninomiya, M., Kunugi, H. and Hashido, K. (2010) Glucocorticoid attenuates brain-derived neurotrophic factor-dependent upregulation of glutamate receptors via the suppression of microRNA-132 expression. *Neuroscience*, **165**, 1301–1311.
54. Cheng, H.Y., Papp, J.W., Varlamova, O., Dziema, H., Russell, B., Curfman, J.P., Nakazawa, T., Shimizu, K., Okamura, H., Impey, S. *et al.* (2007) microRNA modulation of circadian-clock period and entrainment. *Neuron*, **54**, 813–829.
55. Alvarez-Saavedra, M., Antoun, G., Yanagiya, A., Oliva-Hernandez, R., Cornejo-Palma, D., Perez-Iratxeta, C., Sonenberg, N. and Cheng, H.Y. (2011) miRNA-132 orchestrates chromatin remodeling and translational control of the circadian clock. *Hum. Mol. Genet.*, **20**, 731–751.
56. Mellios, N., Sugihara, H., Castro, J., Banerjee, A., Le, C., Kumar, A., Crawford, B., Strathmann, J., Tropea, D., Levine, S.S. *et al.* (2011) miR-132, an experience-dependent microRNA, is essential for visual cortex plasticity. *Nat. Neurosci.*, **14**, 1240–1242.
57. Tognini, P., Putignano, E., Coatti, A. and Pizzorusso, T. (2011) Experience-dependent expression of miR-132 regulates ocular dominance plasticity. *Nat. Neurosci.*, **14**, 1237–1239.
58. Abramov, E., Dolev, I., Fogel, H., Ciccotosto, G.D., Ruff, E. and Slutsky, I. (2009) Amyloid-beta as a positive endogenous regulator of release probability at hippocampal synapses. *Nat. Neurosci.*, **12**, 1567–1576.
59. Li, S., Hong, S., Shepardson, N.E., Walsh, D.M., Shankar, G.M. and Selkoe, D. (2009) Soluble oligomers of amyloid beta protein facilitate hippocampal long-term depression by disrupting neuronal glutamate uptake. *Neuron*, **62**, 788–801.
60. Buckner, R.L., Snyder, A.Z., Shannon, B.J., LaRossa, G., Sachs, R., Fotenos, A.F., Sheline, Y.I., Klunk, W.E., Mathis, C.A., Morris, J.C. *et al.* (2005) Molecular, structural, and functional characterization of Alzheimer's disease: evidence for a relationship between default activity, amyloid, and memory. *J. Neurosci.*, **25**, 7709–7717.
61. Forlenza, O.V., Diniz, B.S. and Gattaz, W.F. (2010) Diagnosis and biomarkers of predementia in Alzheimer's disease. *BMC Med.*, **8**, 89.
62. Forlenza, O.V., Diniz, B.S., Teixeira, A.L., Ojopi, E.B., Talib, L.L., Mendonca, V.A., Izzo, G. and Gattaz, W.F. (2010) Effect of brain-derived neurotrophic factor Val66Met polymorphism and serum levels on the progression of mild cognitive impairment. *World J. Biol. Psychiatry*, **11**, 774–780.
63. Forlenza, O.V., Diniz, B.S., Talib, L.L., Radanovic, M., Yassuda, M.S., Ojopi, E.B. and Gattaz, W.F. (2010) Clinical and biological predictors of

Alzheimer's disease in patients with amnestic mild cognitive impairment. *Rev. Bras. Psiquiatr.*, **32**, 216–222.
64. Laske, C., Stransky, E., Leyhe, T., Eschweiler, G.W., Maetzler, W., Wittorf, A., Soekadar, S., Richartz, E., Koehler, N., Bartels, M. *et al.* (2007) BDNF serum and CSF concentrations in Alzheimer's disease, normal pressure hydrocephalus and healthy controls. *J. Psychiatr. Res.*, **41**, 387–394.
65. Lee, J.G., Shin, B.S., You, Y.S., Kim, J.E., Yoon, S.W., Jeon, D.W., Baek, J.H., Park, S.W. and Kim, Y.H. (2009) Decreased serum brain-derived neurotrophic factor levels in elderly Korean with dementia. *Psychiatry Investig.*, **6**, 299–305.
66. Li, G., Peskind, E.R., Millard, S.P., Chi, P., Sokal, I., Yu, C.E., Bekris, L.M., Raskind, M.A., Galasko, D.R. and Montine, T.J. (2009) Cerebrospinal fluid concentration of brain-derived neurotrophic factor and cognitive function in non-demented subjects. *PLoS One*, **4**, e5424.
67. Zhang, J., Sokal, I., Peskind, E.R., Quinn, J.F., Jankovic, J., Kenney, C., Chung, K.A., Millard, S.P., Nutt, J.G. and Montine, T.J. (2008) CSF multianalyte profile distinguishes Alzheimer and Parkinson diseases. *Am. J. Clin. Pathol.*, **129**, 526–529.
68. Impey, S., Davare, M., Lasiek, A., Fortin, D., Ando, H., Varlamova, O., Obrietan, K., Soderling, T.R., Goodman, R.H. and Wayman, G.A. (2010) An activity-induced microRNA controls dendritic spine formation by regulating Rac1-PAK signaling. *Mol. Cell. Neurosci.*, **43**, 146–156.
69. Hansen, K.F., Sakamoto, K., Wayman, G.A., Impey, S. and Obrietan, K. (2010) Transgenic miR132 alters neuronal spine density and impairs novel object recognition memory. *PLoS One*, **5**, e15497.
70. Pathania, M., Torres-Reveron, J., Yan, L., Kimura, T., Lin, T.V., Gordon, V., Teng, Z.Q., Zhao, X., Fulga, T.A., Van Vactor, D. *et al.*. (2012) miR-132 enhances dendritic morphogenesis, spine density, synaptic integration, and survival of newborn olfactory bulb neurons. *PLoS One*, **7**, e38174.
71. Li, Z., Jo, J., Jia, J.M., Lo, S.C., Whitcomb, D.J., Jiao, S., Cho, K. and Sheng, M. (2010) Caspase-3 activation via mitochondria is required for long-term depression and AMPA receptor internalization. *Cell*, **141**, 859–871.
72. Klein, M.E., Lioy, D.T., Ma, L., Impey, S., Mandel, G. and Goodman, R.H. (2007) Homeostatic regulation of MeCP2 expression by a CREB-induced microRNA. *Nat. Neurosci.*, **10**, 1513–1514.
73. Im, H.I., Hollander, J.A., Bali, P. and Kenny, P.J. (2010) MeCP2 controls BDNF expression and cocaine intake through homeostatic interactions with microRNA-212. *Nat. Neurosci.*, **13**, 1120–1127.
74. Smith, P.Y., Delay, C., Girard, J., Papon, M.A., Planel, E., Sergeant, N., Buee, L. and Hebert, S.S. (2011) MicroRNA-132 loss is associated with tau exon 10 inclusion in progressive supranuclear palsy. *Hum. Mol. Genet.*, **20**, 4016–4024.
75. Min, S.W., Cho, S.H., Zhou, Y., Schroeder, S., Haroutunian, V., Seeley, W.W., Huang, E.J., Shen, Y., Masliah, E., Mukherjee, C. *et al.* (2010) Acetylation of tau inhibits its degradation and contributes to tauopathy. *Neuron*, **67**, 953–966.
76. Shaked, I., Meerson, A., Wolf, Y., Avni, R., Greenberg, D., Gilboa-Geffen, A. and Soreq, H. (2009) MicroRNA-132 potentiates cholinergic anti-inflammatory signaling by targeting acetylcholinesterase. *Immunity*, **31**, 965–973.
77. Blalock, E.M., Geddes, J.W., Chen, K.C., Porter, N.M., Markesbery, W.R. and Landfield, P.W. (2004) Incipient Alzheimer's disease: microarray correlation analyses reveal major transcriptional and tumor suppressor responses. *Proc. Natl Acad. Sci. USA*, **101**, 2173–2178.
78. Bronner, I.F., Bochdanovits, Z., Rizzu, P., Kamphorst, W., Ravid, R., van Swieten, J.C. and Heutink, P. (2009) Comprehensive mRNA expression profiling distinguishes tauopathies and identifies shared molecular pathways. *PLoS One*, **4**, e6826.
79. Qin, W., Zhao, W., Ho, L., Wang, J., Walsh, K., Gandy, S. and Pasinetti, G.M. (2008) Regulation of forkhead transcription factor FoxO3a contributes to calorie restriction-induced prevention of Alzheimer's disease-type amyloid neuropathology and spatial memory deterioration. *Ann. N. Y. Acad. Sci.*, **1147**, 335–347.
80. Picone, P., Giacomazza, D., Vetri, V., Carrotta, R., Militello, V., San Biagio, P.L. and Di Carlo, M. (2011) Insulin-activated Akt rescues Abeta oxidative stress-induced cell death by orchestrating molecular trafficking. *Aging Cell*, **10**, 832–843.
81. Shang, Y.C., Chong, Z.Z., Hou, J. and Maiese, K. (2009) The forkhead transcription factor FOXO3a controls microglial inflammatory activation and eventual apoptotic injury through caspase 3. *Curr. Neurovasc. Res.*, **6**, 20–31.
82. Engidawork, E., Gulesserian, T., Seidl, R., Cairns, N. and Lubec, G. (2001) Expression of apoptosis related proteins in brains of patients with Alzheimer's disease. *Neurosci. Lett.*, **303**, 79–82.
83. Biswas, S.C., Shi, Y., Vonsattel, J.P., Leung, C.L., Troy, C.M. and Greene, L.A. (2007) Bim is elevated in Alzheimer's disease neurons and is required for beta-amyloid-induced neuronal apoptosis. *J. Neurosci.*, **27**, 893–900.
84. Morishima, Y., Gotoh, Y., Zieg, J., Barrett, T., Takano, H., Flavell, R., Davis, R.J., Shirasaki, Y. and Greenberg, M.E. (2001) Beta-amyloid induces neuronal apoptosis via a mechanism that involves the c-Jun N-terminal kinase pathway and the induction of Fas ligand. *J. Neurosci.*, **21**, 7551–7560.
85. Su, J.H., Anderson, A.J., Cribbs, D.H., Tu, C., Tong, L., Kesslack, P. and Cotman, C.W. (2003) Fas and Fas ligand are associated with neuritic degeneration in the AD brain and participate in beta-amyloid-induced neuronal death. *Neurobiol. Dis.*, **12**, 182–193.
86. Kim, W.S., Bhatia, S., Elliott, D.A., Agholme, L., Kagedal, K., McCann, H., Halliday, G.M., Barnham, K.J. and Garner, B. (2010) Increased ATP-binding cassette transporter A1 expression in Alzheimer's disease hippocampal neurons. *J. Alzheimers Dis.*, **21**, 193–205.